Impact Analysis of Mast Tower

A Report Submitted by

Rhythm Sharma

Contents

List of Figures

Impact Analysis of Mass Tower

1 Introduction

Impact loading is one of the most critical conditions that engineering structures may encounter during their service life. Structures such as towers, plates, and aerospace components are often subjected to high-velocity impacts caused by accidental collisions, debris, or moving objects. Understanding the structural behavior of such systems under dynamic impact conditions is essential for designing safe and reliable structures.

This project focuses on two distinct impact scenarios involving structures. The first case studies the impact of a bullet on a plate, representing a localized, high-velocity impact problem. The second case investigates the collision between an aircraft wing (impactor) and a mass tower, representing a large-scale structural impact scenario. These two cases allow the analysis of different modes of deformation, stress distribution, and energy transformation under varying magnitudes of dynamic loads.

The simulations have been performed using **ANSYS Workbench**, the **inbuilt LS-DYNA solver**, and **LS-PrePost** for post-processing. These software tools enable the modeling of transient impact events with high accuracy, accounting for nonlinear material behavior, contact interactions, and energy dissipation mechanisms. The study primarily evaluates parameters such as kinetic energy, internal energy, total energy, and rigid body displacement to understand the response and performance of structures under impact loading.

1.1 Governing Equation

The dynamic response of a structure subjected to impact loading is governed by the time-dependent equation of motion derived from Newton's Second Law. In matrix form, the equation for a discretized finite element system is expressed as:

$$\mathbf{M}\ddot{\mathbf{u}}(t) + \mathbf{C}\dot{\mathbf{u}}(t) + \mathbf{K}\mathbf{u}(t) = \mathbf{F}_{ext}(t) \tag{1}$$

In this equation:

1. $\mathbf{M}$ is the global mass matrix and represents the inertia of the structure, resisting any change in acceleration.
2. $\mathbf{C}$ is the damping matrix, accounting for energy dissipation through internal friction or external resistance.
3. $\mathbf{K}$ is the stiffness matrix, governing the restoring elastic forces developed due to deformation.
4. $\mathbf{u}(t)$, $\dot{\mathbf{u}}(t)$, and $\ddot{\mathbf{u}}(t)$ are the displacement, velocity, and acceleration vectors at time t, respectively.
5. $\mathbf{F}_{ext}(t)$ represents the external force vector applied to the structure, which, in this study, corresponds to the impulsive load generated during the impact event.

This equation indicates that the inertia, damping, and elastic restoring forces must collectively balance the externally applied impact forces at every instant. In static loading these contributions are negligible, but during high-velocity impact the rapid acceleration and large strain rates make inertia and damping effects dominant. Therefore, all terms of the governing equation are essential for accurately capturing the transient behavior of the structure.

1.1.1 Explicit Time Integration Scheme in LS-DYNA

In LS-DYNA, the above equation of motion is solved using the **explicit central difference method**, which is particularly efficient for solving high-speed impact, crash, or blast simulations. The method computes nodal accelerations and updates velocities and displacements incrementally as follows:

$$\ddot{\mathbf{u}}_t = \mathbf{M}^{-1}(\mathbf{F}_{ext,t} - \mathbf{F}_{int,t}) \tag{2}$$

$$\dot{\mathbf{u}}_{t+\frac{\Delta t}{2}} = \dot{\mathbf{u}}_{t-\frac{\Delta t}{2}} + \Delta t\, \ddot{\mathbf{u}}_t \tag{3}$$

$$\mathbf{u}_{t+\Delta t} = \mathbf{u}_t + \Delta t\, \dot{\mathbf{u}}_{t+\frac{\Delta t}{2}} \tag{4}$$

This explicit scheme does not require inversion of the stiffness matrix, making it computationally efficient for problems involving highly nonlinear behavior, large deformations, and complex contact interactions. However, the stability of the explicit method is conditional and requires that the time step Δt be smaller than a critical value defined by the Courant–Friedrichs–Lewy (CFL) condition:

$$\Delta t_{crit} < \frac{L_{min}}{c} \tag{5}$$

where L_{min} is the smallest characteristic element length, and c is the dilatational wave speed of the material.

1.2 Impact Analysis

Impact analysis is essential for understanding how structural components behave under sudden, high-velocity loading. Such situations commonly occur in real-life scenarios including projectile impact on metallic walls or accidental collision of moving bodies with fixed support structures. The present study considers two representative impact cases that reflect both localized and global impact responses.

1.2.1 Impact of wing on Mast Tower

This case represents a larger-scale structural impact comparable to scenarios where an aircraft wing or a moving structural component strikes a communication mast or slender tower. Such incidents may occur near airfields, industrial plants, or tall installation sites. The objective is to understand the global deformation and stability of the tower during an impulsive horizontal impact.

Figure 1.1 shows the tower geometry developed in ANSYS Workbench with its assigned cross-sections. The impactor model representing an aircraft wing is shown in Figure 1.2.

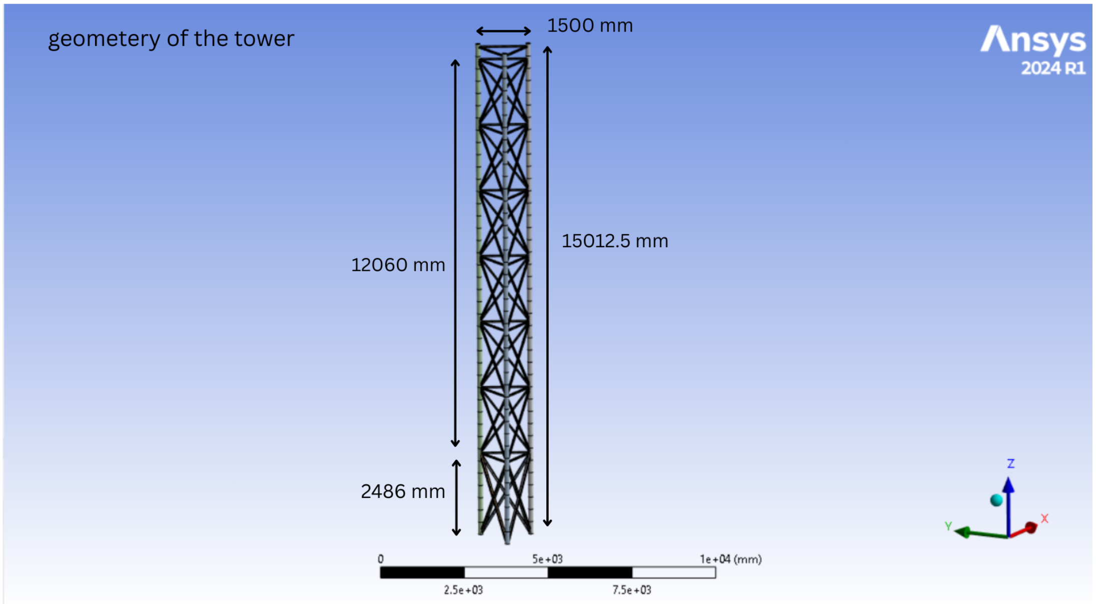

Figure 1.1: Geometry of the mast tower created in ANSYS Workbench with cross-sections.

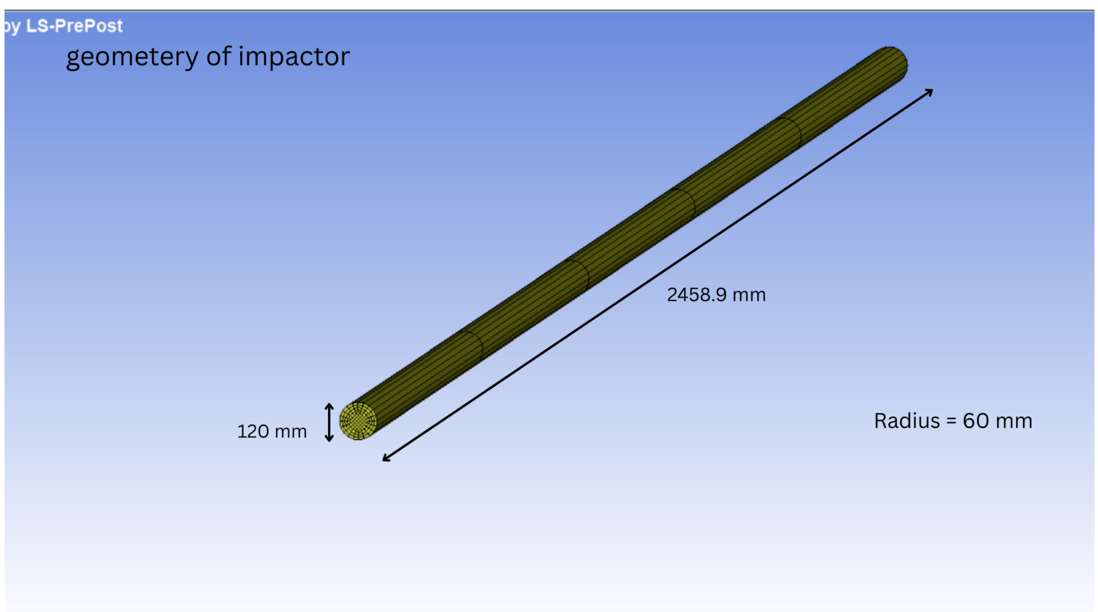

Figure 1.2: Impactor (wing model) used for the mast tower collision analysis.

2 Problem Statement

2.1 Impact of wing on Mast Tower

2.1.1 Problem definition

This case examines the dynamic response of a slender mast tower subjected to a horizontal impact by a rigid impactor representing an aircraft wing. The objectives are (1) to evaluate global deformation and displacement histories of the tower under impulsive loading, (2) to identify velocity conditions that lead to significant permanent deformation or loss of integrity, and (3) to study energy absorption characteristics through kinetic, internal and total energy histories.

2.1.2 Geometry and cross-section definitions

The geometric and cross-section parameters used for the mast tower model are listed below.

1. Overall geometry:
   (a) Total tower height: 15012.5 mm.
   (b) Lower most segment length : 2486 mm.
   (c) width of the tower (in xy plane): 1500 mm.
2. Cross-sections:
   (a) Rectangular tube cross-section : outer rectangle 41 $mm \times 41$ mm; inner rectangle 33 $mm \times$ 33 mm.
   (b) Rectangular tube cross-section : outer rectangle 63 $mm \times 63$ mm; inner rectangle 51 $mm \times$ 51 mm.
   (c) Circular tube: outer radius 75 mm; inner radius 69 mm.
3. Materials and element types:
   (a) Tower material: aluminium, modelled using MAT_024 (piecewise linear plasticity)
   (b) Impactor: solid cylinder, rigid body, radius 60 mm, length 2458.9 mm.
   (c) Finite Element detials: The tower model is discretised using line and beam elements, resulting in a total of 1,884 elements and 3,726 nodes.

   The wing (impactor) model is meshed using solid elements, with 525 elements and 696 nodes. The computed surface area of the wing is 1.88277×10^6 mm^2, and the corresponding volume is 2.78113×10^7 mm^3. This level of

2.1.3 Boundary conditions, contact and loading

1. A fixed support is been given to the base of the tower

2. Contact definitions: automatic node-to-surface and automatic beam-to-surface contact are used between the rigid Impactor and tower members.

3. Velocity : the impactor is moving with a initial horizontal velocity of 10 m/s (in LS-PrePost). Additional visualisation cases are prepared at impact speeds corresponding to 140 km/h, 80 km/h and 50 km/h (approximately 38.9 m/s, 22.2 m/s and 13.9 m/s) (in LS-DYNA WorkBench).

2.1.4 Cross-section Figures

In this subsection, the three cross-sections used in the tower model are presented. Figure 2.1 shows the first rectangular tube section with an out rectangle of 41 mm*41 mm and an inner rectangle of 33 mm*33 mm. Figure 2.2 illustrates the second rectangular tube section with an outer rectangle of 63 mm*63 mm and an inner rectangle of 51 mm*51 mm. Figure 2.3 shows the circular tube section, having an inner radius of 69 mm and an outer radius of 75 mm.

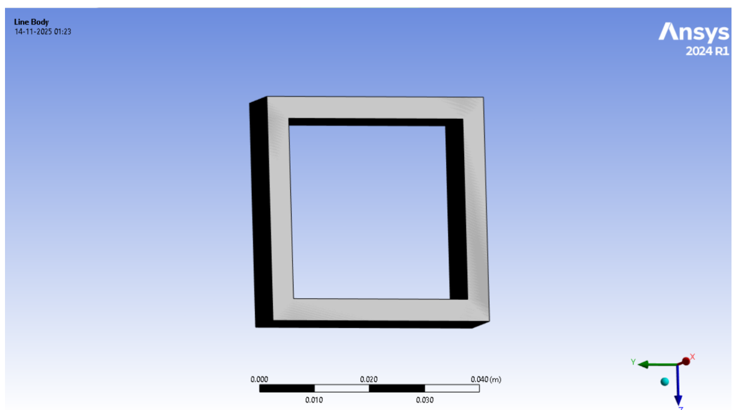

Figure 2.1: Rectangular cross-section with 41 mm outer (inner 33 mm).

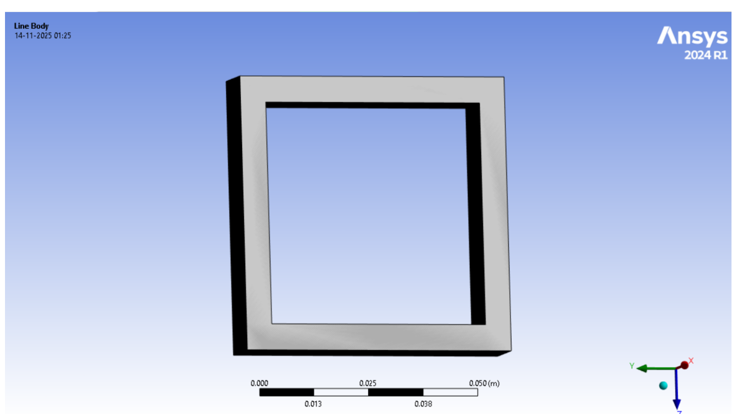

Figure 2.2: Rectangular cross-section with 63 mm outer (inner 51 mm).

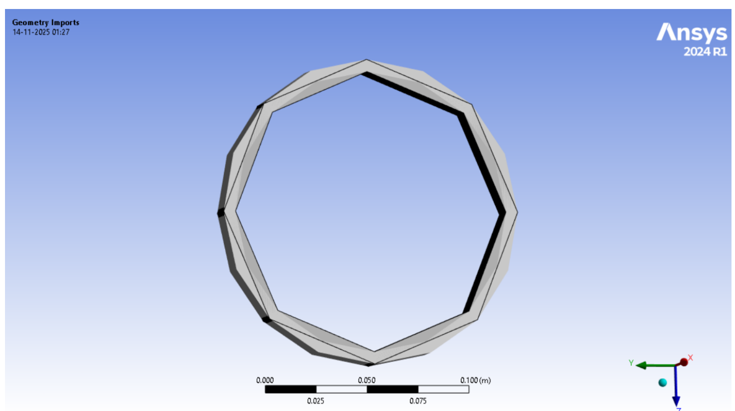

Figure 2.3: Circular tube cross-section with inner radius 69 mm and outer radius 75 mm.

2.2 Impact of wing on Mast Tower

This section presents the results of the impact between the aircraft wing (rigid impactor) and the Tower.

2.2.1 Visualisation of impact of wing on the tower

The deformation progression of the aluminium tower during the wing impact at different time frames is shown below. The sequence clearly captures the approach of the rigid wing, initial contact, progressive bending of the tower, peak lateral deformation in the mid-section, and the final permanently deformed also we have added workbench and LS-Prepost images at three different speeds that is at 50 kmph , 80 kmph and 140 kmph .

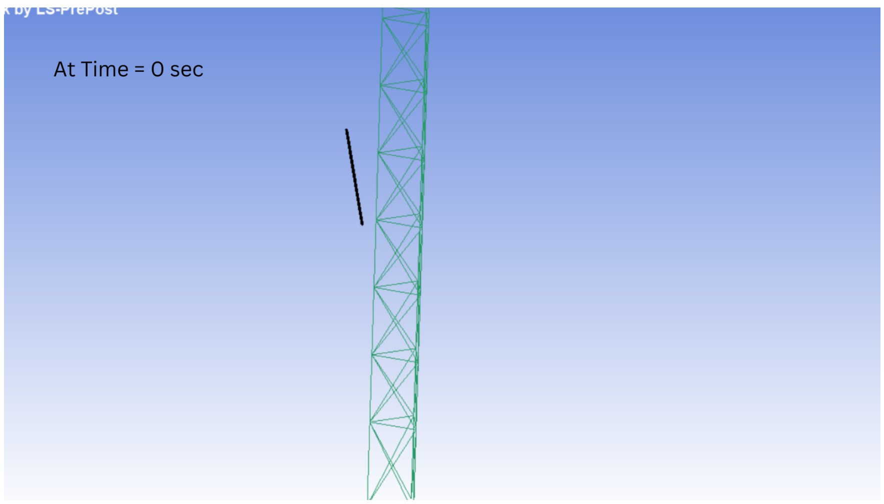

Impact of wing on tower at velocity = 36 kmph and $t = 0$ sec

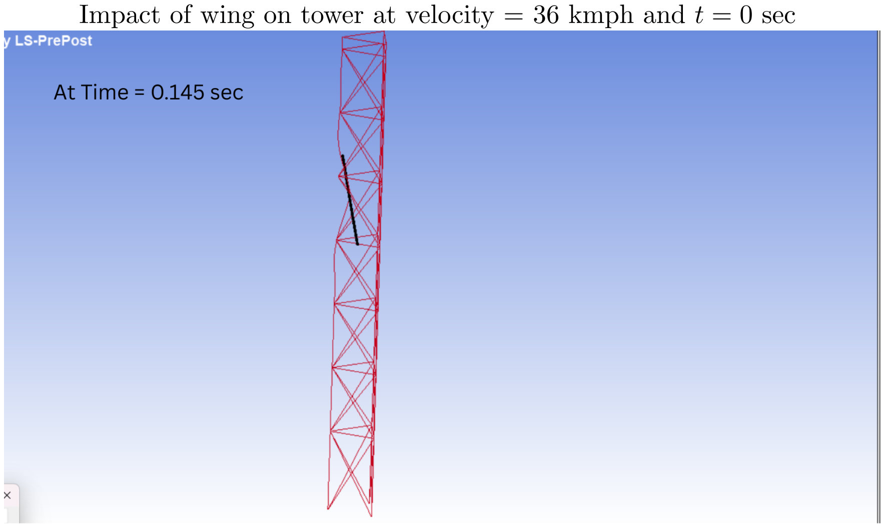

Impact of wing on tower at velocity = 36 kmph and $t = 0.145$ sec

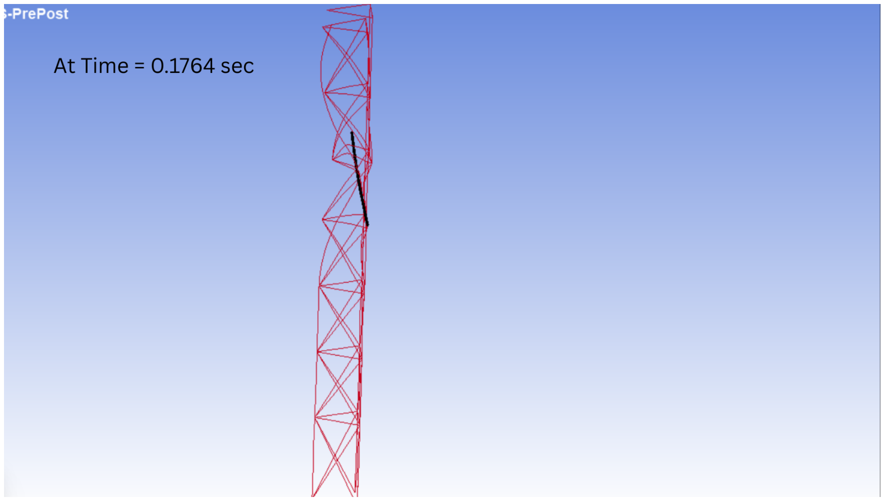

Impact of wing on tower at velocity = 36 kmph and $t = 0.1764$ sec

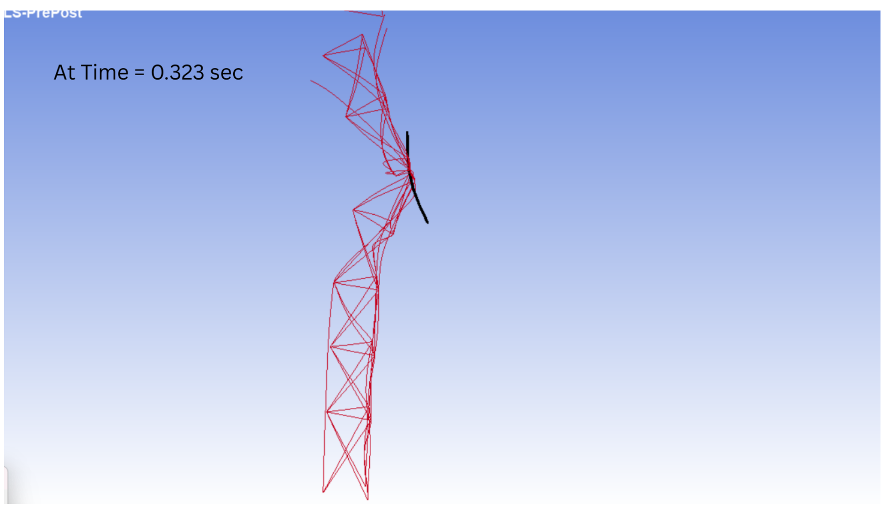

Impact of wing on tower at velocity = 36 kmph and $t = 0.323$ sec

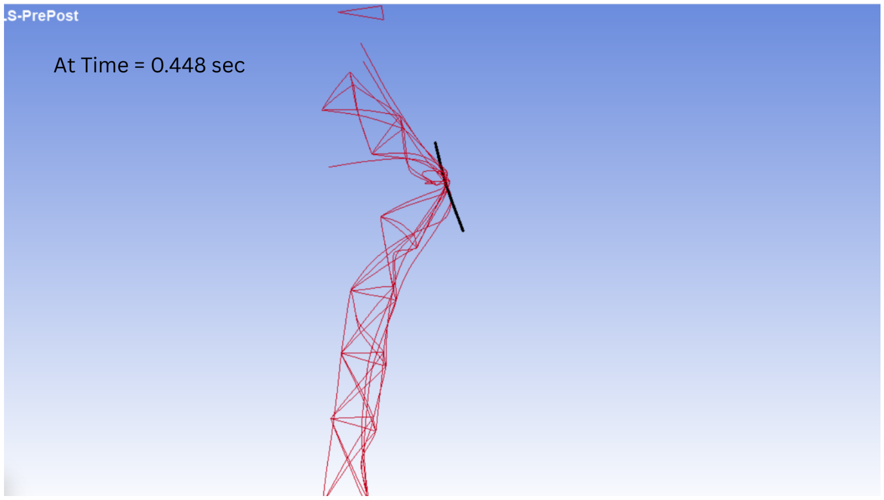

Impact of wing on tower at velocity = 36 kmph and $t = 0.448$ sec

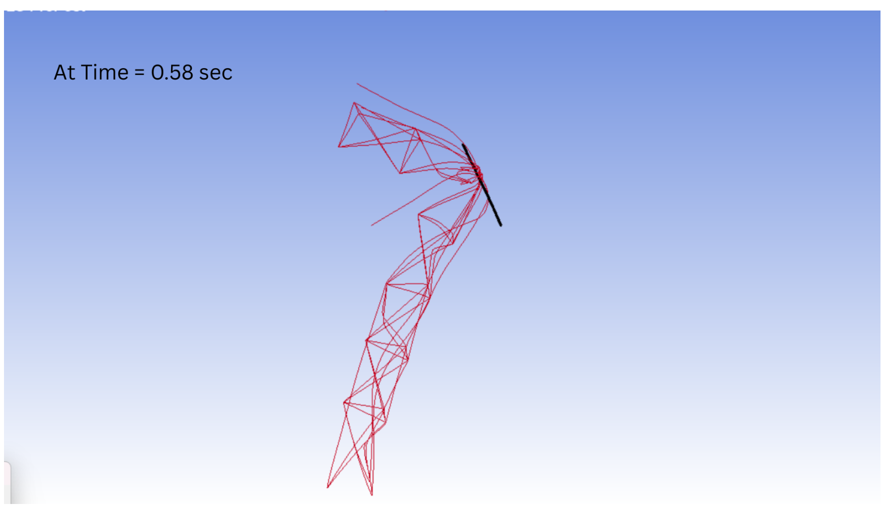

Impact of wing on tower at velocity = 36 kmph and $t = 0.58$ sec

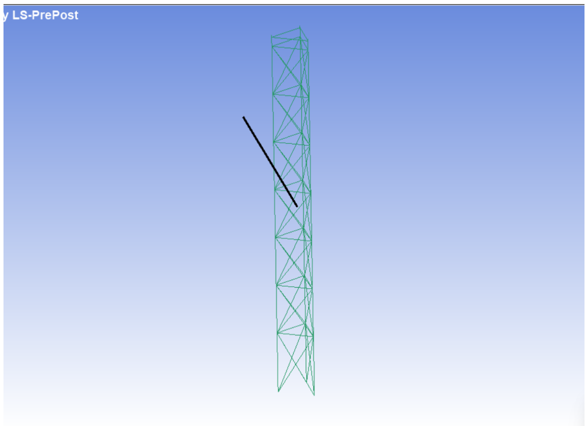

Figure 2.4: Impact at v = 50 km/h and t = 0.028 sec

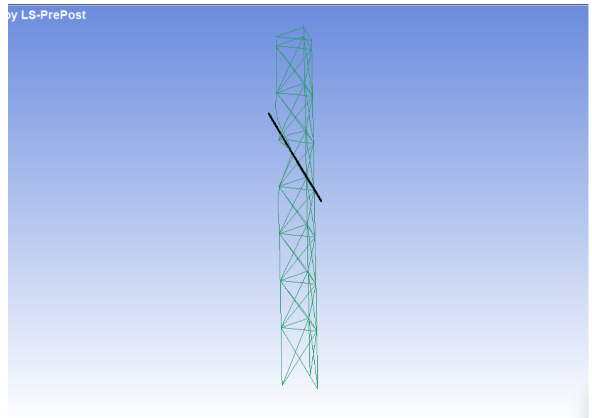

Figure 2.5: Impact at v = 50 km/h and t = 0.088 sec

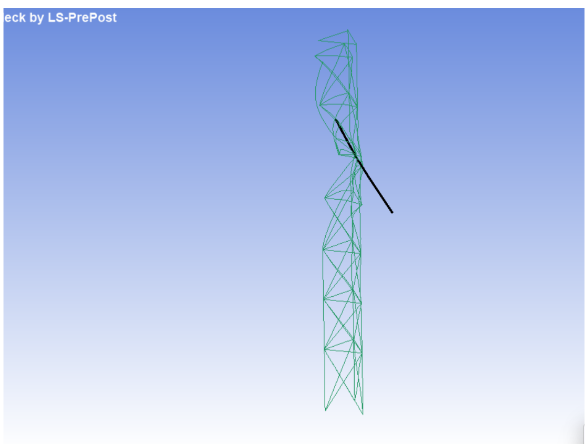

Figure 2.6: Impact at v = 50 km/h and t = 0.1583 sec

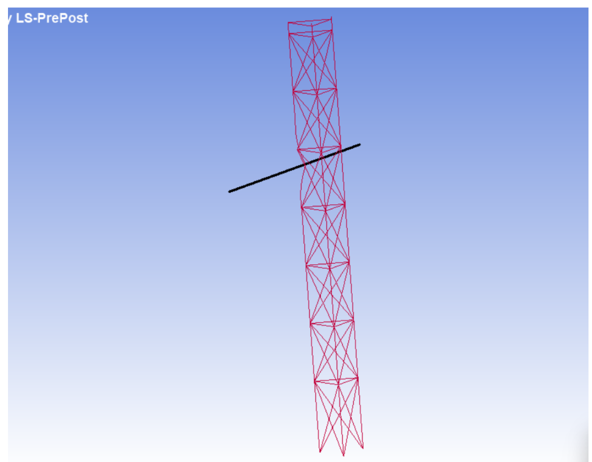

Figure 2.7: Impact at v = 80 km/h and t = 0.0414 sec

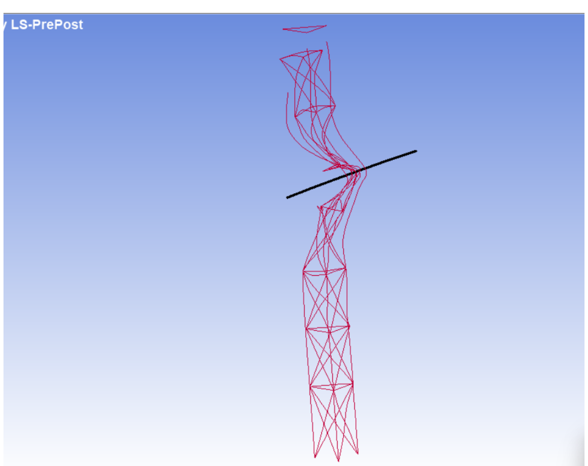

Figure 2.8: Impact at v = 80 km/h and t = 0.148 sec

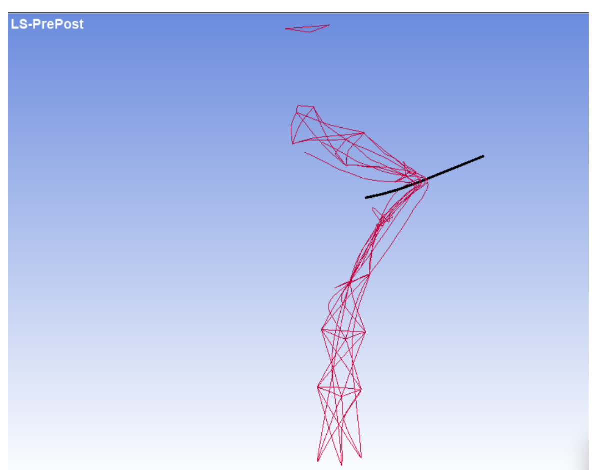

Figure 2.9: Impact at v = 80 km/h and t = 0.28 sec

Figure 2.10: **Impact deformation progression at 50 and 80 km/h at different time frames**

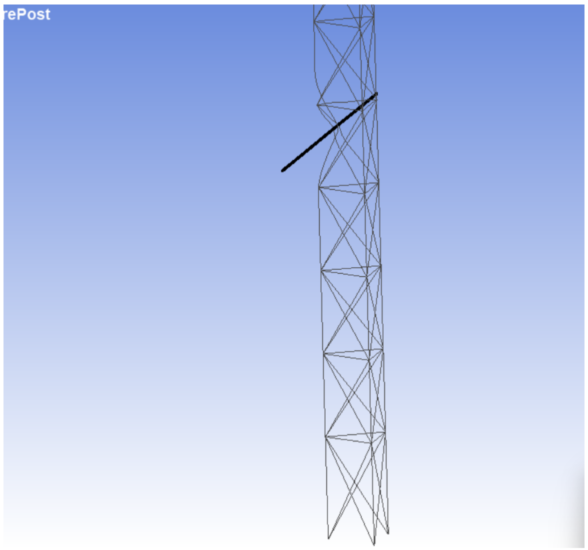

Figure 2.11: Impact at v = 140 km/h and t = 0.030 sec

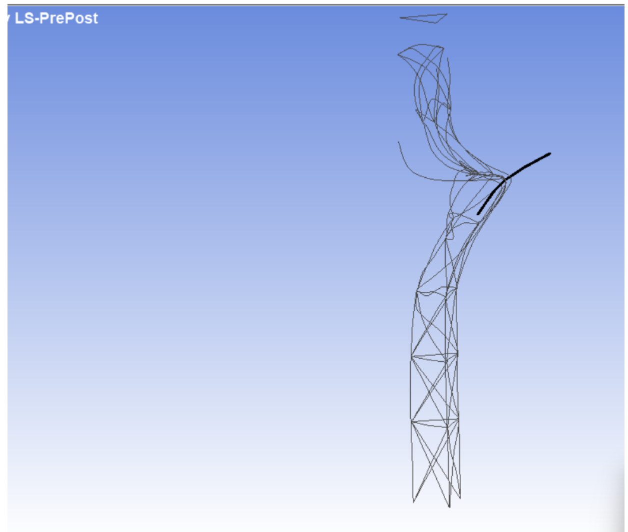

Figure 2.12: Impact at v = 140 km/h and t = 0.108 sec

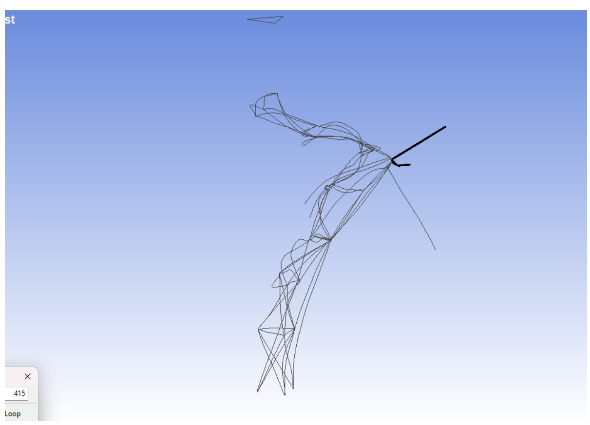

Figure 2.13: Impact at v = 140 km/h and t = 0.20 sec

Figure 2.14: **Impact deformation progression of mast tower at 140 km/h and different time frames**

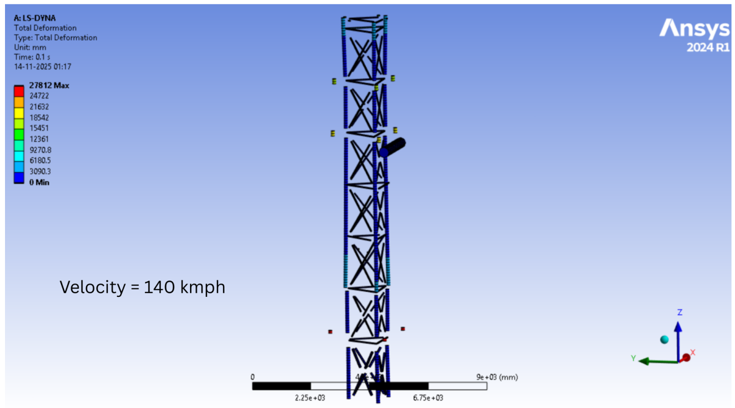

Figure 2.15: Impact of wing on tower at velocity 140 km/h ($\approx 38.9\ m/s$)

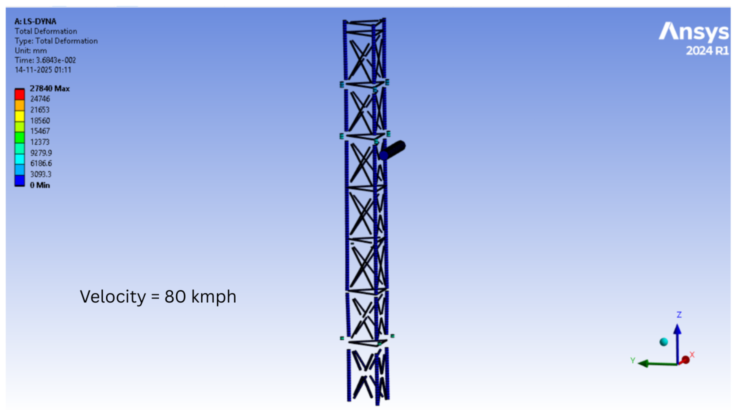

Figure 2.16: Impact of wing on tower at velocity 80 km/h ($\approx 22.2\ m/s$)

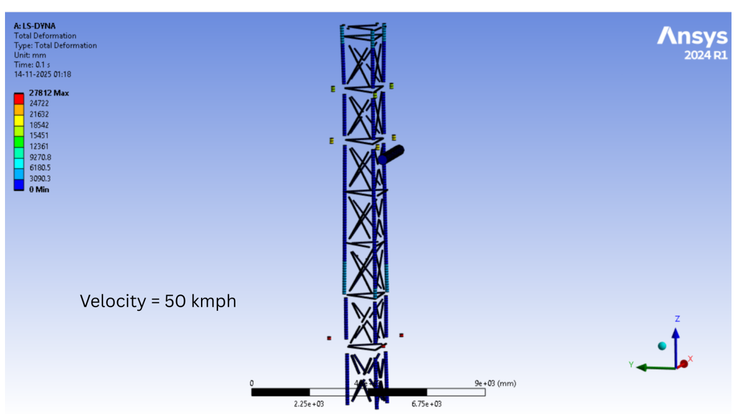

Figure 2.17: Impact of wing on tower at velocity 50 km/h ($\approx 13.9\ m/s$)

Figure 2.18: ANSYS Workbench visualisations of tower–impactor interaction at three representative speeds.

2.2.2 Internal Energy

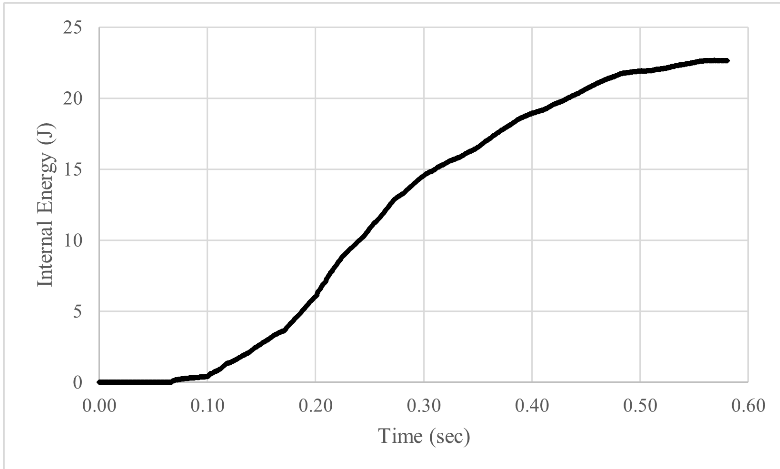

Figure 2.19: Internal energy variation of the tower during wing impact at 36 kmph.

The tower internal energy rises rapidly after the impact and reaches a maximum value of nearly **2.25 $\times$ $\mathbf{10^6}$ units**. The steep rise signifies severe plastic deformation in the lower and middle cross–sections of the tower. After **0.40–0.45 s**, the curve becomes stable, indicating that the major deformation process has finished and the structure has reached a post–impact equilibrium state.

2.2.3 Kinetic Energy

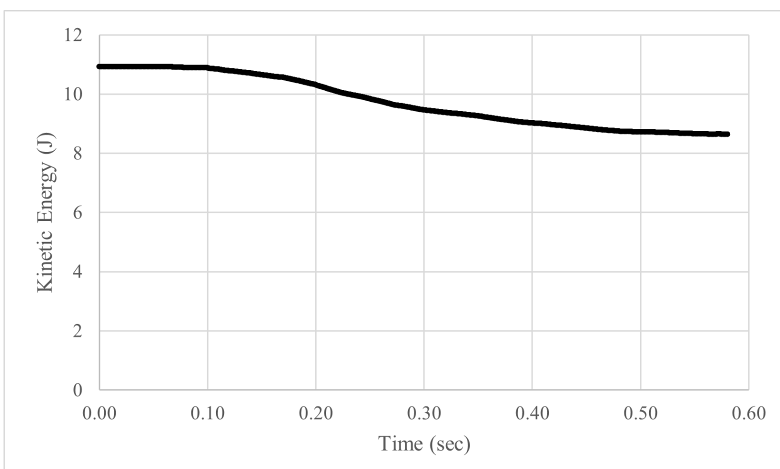

Figure 2.20: Kinetic energy decay of the impactor during tower strike at 36 kmph.

The impactor begins with a kinetic energy of approximately **1.15 $\times$ $\mathbf{10^7}$ units**. As the wing strikes the tower, the kinetic energy decreases steadily and drops to about **8.7 $\times$ $\mathbf{10^6}$** by the end of the simulation. This reduction confirms energy absorption by the tower in the form of plastic deformation. The smooth decay indicates controlled deformation without numerical instability.

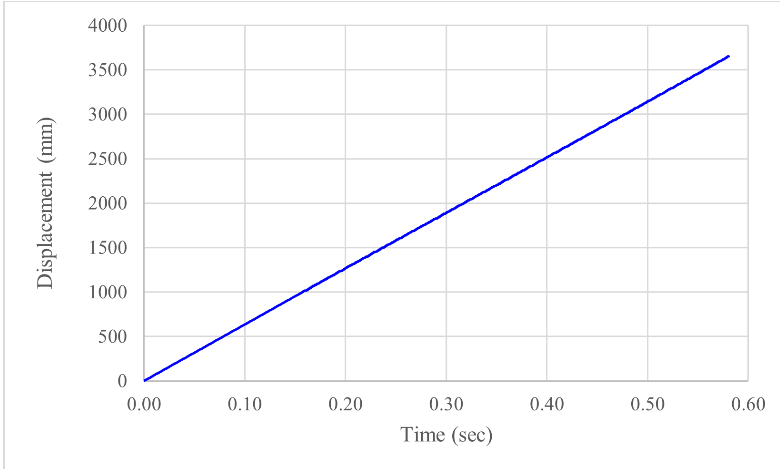

Figure 2.21: Resultant displacement of the tower during impact at 36 kmph.

2.2.4 Resultant Tower Displacement

The tower displacement increases sharply after impact and reaches a maximum of approximately **6.3 units**. After this peak, the displacement remains nearly constant.

2.2.5 Total Energy

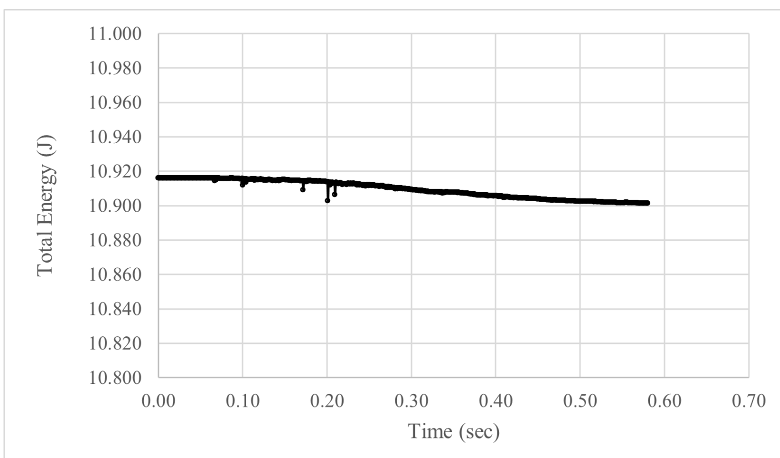

Figure 2.22: Total energy response of the tower–wing system at 36 kmph.

The total energy initially decreases from around $\mathbf{1.2 \times 10^7}$ to approximately $\mathbf{8.5 \times 10^6}$, after which it becomes stable. The early reduction corresponds to the conversion of kinetic energy into internal energy (deformation in tower members).

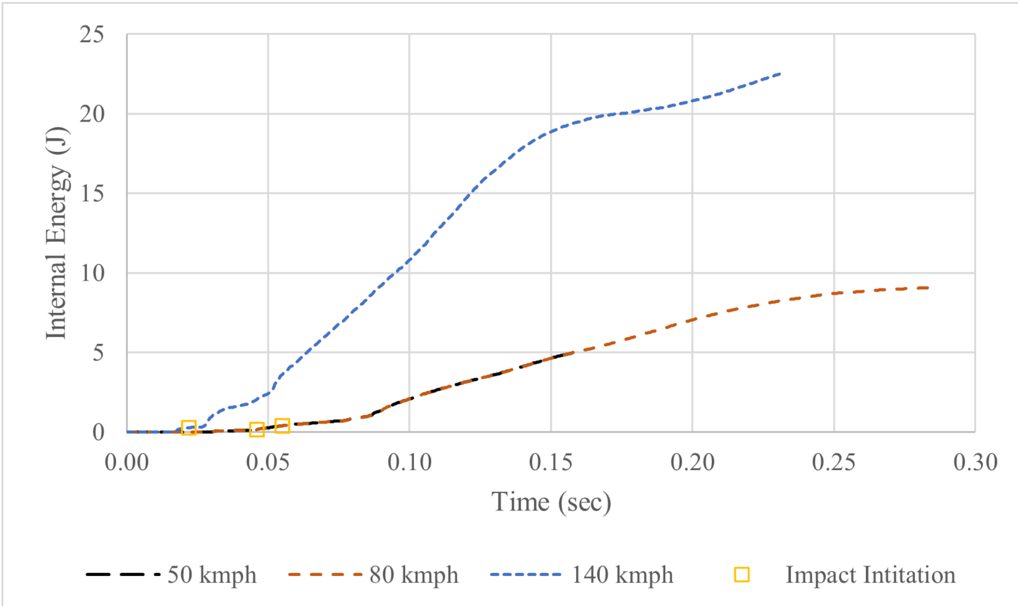

Figure 2.23: Internal energy variation of the tower–wing system at 50, 80, and 140 kmph impact velocities.

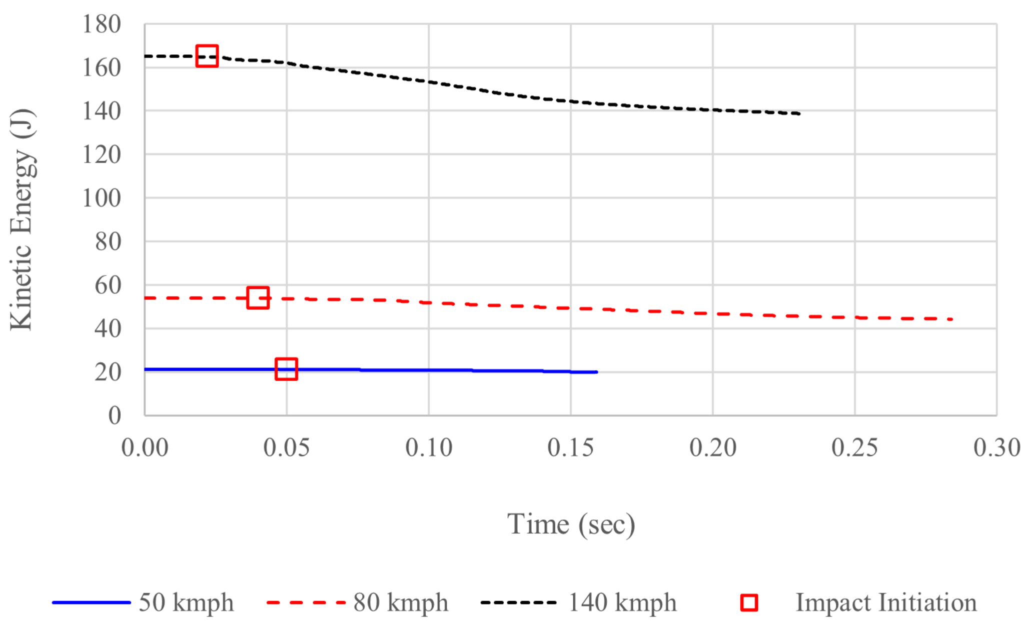

Figure 2.24: Kinetic energy response of the system during impact at 50, 80, and 140 kmph velocities.

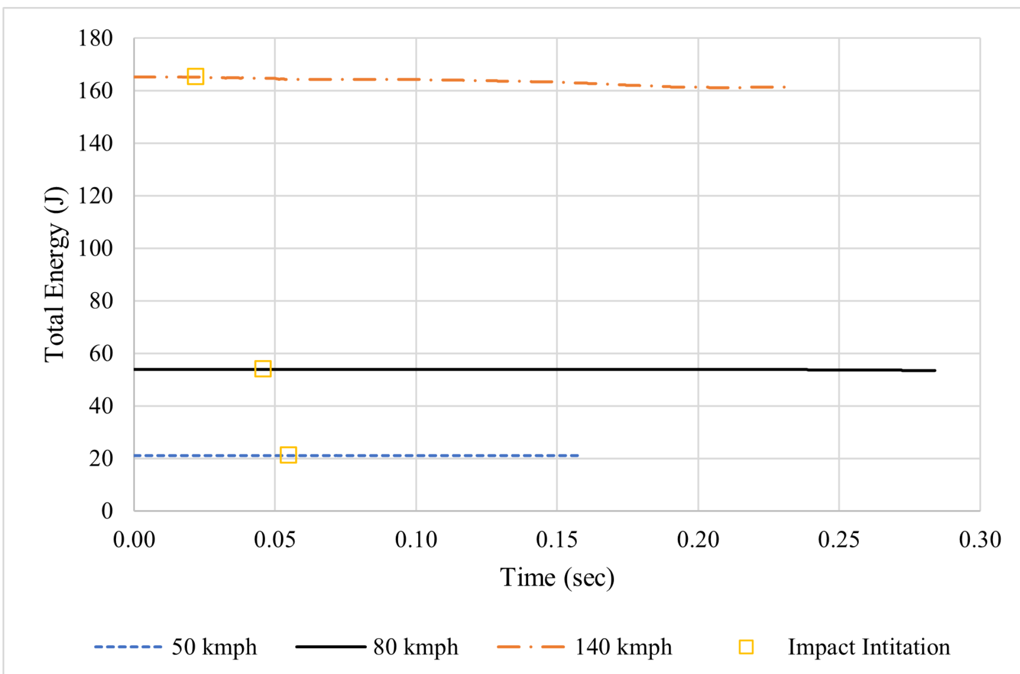

Figure 2.25: Total energy Response of the tower–wing system for different velocities (50, 80, and 140 kmph).